The Fourth IEEE RAS/EMBS International Conference
on Biomedical Robotics and Biomechatronics
Roma, Italy. June 24-27, 2012

Design of Joint Locks for Underactuated Fingers

Bart Peerdeman* , Gert Jan Pieterse*, Stefano Stramigioli*, Hans Rietman*,
Edsko Hekman*, Dannis Brouwer†, and Sarthak Misra*

***Abstract*— Modern multifunctional hand prostheses have many degrees of freedom, but strong limitations on weight and size. The actuators commonly used in these systems are relatively large and heavy, so their number should be kept as low as possible. This is often accomplished by underactuation, which causes a natural motion of the fingers when grasping an object but reduces the ability to execute a variety of grasps. To remedy this, a series of locking mechanisms can be implemented to fix the position of one or more joints. This paper focuses on the development of such a joint locking system that could be used in anthropomorphic prosthetic fingers. Two lock concepts are implemented in a single-joint test setup and evaluated. A gear-based concept is tested, though its actuation requirements prove too high for viable implementation in a prosthesis. A mechanism based on friction amplification is shown to exhibit self-locking properties, which allows for a minimal lock actuation force while withstanding joint torques of over 2 Nm. The friction amplification mechanism is found suitable for prosthesis use, and will be developed further for implementation in a future prosthesis prototype.**

I. Introduction

Modern electrically powered hand prostheses [1], [2], [3] emulate the structure of the human hand for both cosmetic and practical reasons. The human hand has over 20 degrees of freedom (DOFs), but imposes strong restrictions on the size and weight of an anthropomorphic prosthesis.

DC motors are currently the preferred method of actuation for both commercial and prototype hand prostheses [4]. These actuators are versatile, easily controlled, and readily available. However, the size and weight of the motors and their transmissions allow only a few to be placed inside the prosthesis. This limitation is circumvented by modern prostheses in various ways, shown in Figure 1.

These underactuation techniques all allow a single motor to actuate multiple DOFs. However, they also reduce the individual controllability of these DOFs. Mechanisms to transfer the actuation torque of a single motor to different joints have been implemented to remedy this [5], though this approach is limited to small numbers of DOFs. Alternatively, some robotic and prosthetic hands have included passive mechanisms to block joints or entire fingers when certain external forces or torques are applied [6], [7].

The ability to actively lock and release joints can be used to change underactuated fingers' flexion trajectory, or to selectively actuate combinations of fingers with a single actuator. In this paper, novel miniature locking mechanisms are developed to actively control individual joint movement in tendon-pulley underactuated fingers. These mechanisms can fit inside of the phalanges, leading to the development of smaller and lighter multifunctional hand prostheses.

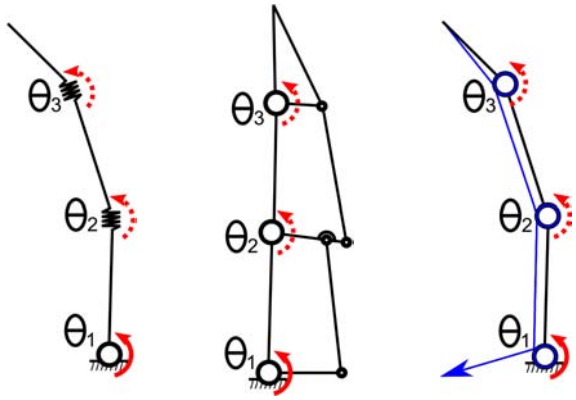

Fig. 1. Various implementations of underactuation in prosthetic hands: (a) passive elements replacing actuated joints [8], (b) mechanically linked joints/fingers [9], and (c) tendon-pulley mechanisms [10]. The joint angles θ_1, θ_2, and θ_3 are passively connected; actuation of the proximal joint (or in (c), the blue tendon) causes the other joints to move. The actuated joints are represented by solid red arrows, while the passive joints are indicated by dashed red arrows.

The locks' requirements are derived in Section II. Section III describes the different concepts that were explored for both joint locking and actuation. The testing of the various concepts is discussed in Section IV, and in Section V the test results are shown. In Section VI, these results are discussed; Section VII concludes the paper and provides directions for future work.

II. Requirements

Implementation of joint locks in a modern multifunctional hand prosthesis leads to a number of requirements which have to be fulfilled. These requirements will be used to evaluate the lock concepts.

First of all, the joint locks have to be fitted inside a human-sized hand. The smallest finger joint to be individually controllable is the proximal interphalangeal (PIP) joint, which has an average depth and width of approximately 17 mm [11]. Any other mechanisms should fit inside of the proximal phalanx, the average length of which is approximately 30 mm, excluding the joints [12]. Because of this, the joint locks should be designed to be operable with as little force and stroke as possible. An important property to accomplish

* MIRA - Institute for Biomedical Technology and Technical Medicine, University of Twente, The Netherlands.

† CTIT - Centre for Telematics and Information Technology, University of Twente, Netherlands.

This research (Project: MyoPro) is funded by the Dutch Ministry of Economic Affairs and the Province of Overijssel within the Pieken in de Delta (PIDON) initiative.

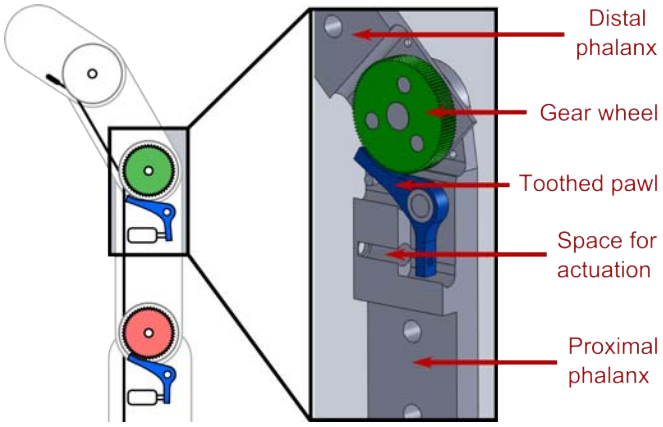

Fig. 2. Gear locking concept. Rotating the toothed pawl locks the joint by blocking the gear wheel connected to the distal phalanx.

this is self-locking, or the ability of a locked, actuated joint to remain locked without applying force to the lock. This significantly reduces the required lock actuation force.

The locks also need to withstand the torque exerted on them by the main actuator. This locking torque is highest when the locks are engaged while grasping an object, which occurs during the tripod grasp. In many modern prostheses, the grasp force for precision grasping lies between 5-10 N [9], [10], [13]. With an average finger length of 100 mm [12], this amounts to a maximum locking torque of 1 Nm on the most proximal finger joint.

III. Concepts

The concepts for joint locking mechanisms can be divided into two main approaches: constraining the joint movement by locking elements; and canceling out the joint torque with an opposing friction force [14]. Each approach has its own drawbacks and advantages, and therefore a mechanism has been designed for each of these approaches.

A. Gear locking

To constrain joint motion, a gear can be rigidly connected to the joint, and movement of the gear can be obstructed by a toothed block. This gear locking concept has been further developed into the mechanism of Figure 2. It consists of a radially toothed gear wheel connected to the distal phalange of the joint and a toothed pawl connected to the proximal phalanx. This pawl can be rotated around its shaft to either lock or release the wheel. In order to avoid overloading of the mechanism and prevent problems with releasing the lock, the teeth do not completely block the motion of the gear; however, the toothed pawl is designed for a high ratio between locking torque and actuation force.

A possible shortcoming of this concept is the indexing resolution caused by the limited number of teeth on the gear wheel. An added requirement of an indexing resolution under 5 degrees was added to the gear concept for this reason.

Design: For the design of the gear wheel and toothed pawl, several properties need to be considered: the number of teeth should be maximized to reduce the indexing resolution, the shape of the teeth should enable self-locking to reduce the required actuation force, and the gear teeth should be strong enough to withstand the maximum joint torque.

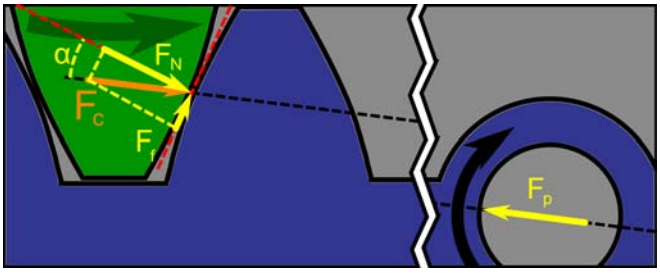

Fig. 3. Gear locking concept free body diagram, illustrating the contact angle α and the forces on the toothed pawl: the friction force F_f, normal force F_N, total contact force F_c, and pawl shaft force F_p. Curved arrows indicate the parts' direction of motion before locking.

At least 72 teeth are required for an indexing resolution below 5 degrees. In this concept 100 teeth were used, which leads to a resolution of 3.6 degrees. Due to manufacturing restrictions, the minimal module for this number of teeth was 0.2 mm, which led to a gear diameter of 20 mm. Though this exceeds the lock size requirement, it provides a proof of concept; a 75-tooth gear fulfils both requirements.

In order to enable self-locking, the teeth should have a contact angle α such that the friction force F_f between the gear wheel and the pawl keeps the teeth together when a constant joint torque is applied (see Figure 3). The static friction depends on the normal force on the pawl F_N as follows:

$$F_f \leqq \mu F_N \tag{1}$$

with μ being the friction coefficient between the pawl and gear. Given a static equilibrium condition, both F_N and F_f can be derived from the pawl shaft force F_p:

$$F_N = -\cos(\alpha)F_p \; ; \; F_f = -\sin(\alpha)F_p \tag{2}$$

This leads to the following relationship for F_f and F_N:

$$F_f = \tan(\alpha)F_N \tag{3}$$

Combining (1) and (3) leads to the conclusion that the pawl should be self-locking if $\tan(\alpha)$ is less than or equal to μ. The contact is steel-on-steel, and a value for μ of approximately 0.4 is expected. In this case, a contact angle of 20 degrees or less should be sufficient to achieve self-locking in most circumstances.

The force on the gear lock is limited by the maximum bending stress on a single tooth. The Lewis equation [15] is a simple method of determining the maximum bending stress on a gear tooth in a static situation. The bending stress σ_b can be determined as follows:

$$\sigma_b = \frac{F_c}{b \cdot m \cdot Y} \tag{4}$$

Here, F_c is the contact force on the tooth in N, b is the tooth width in mm, m is the gear module in mm, and Y is the Lewis Form Factor, which for 100 involute teeth at 20 degrees is 0.447 [15]. For F_c, b, and m being 100 N, 4 mm, and 0.2 mm respectively, σ_b is calculated to be 278 MPa. An allowable bending stress can be estimated at one third

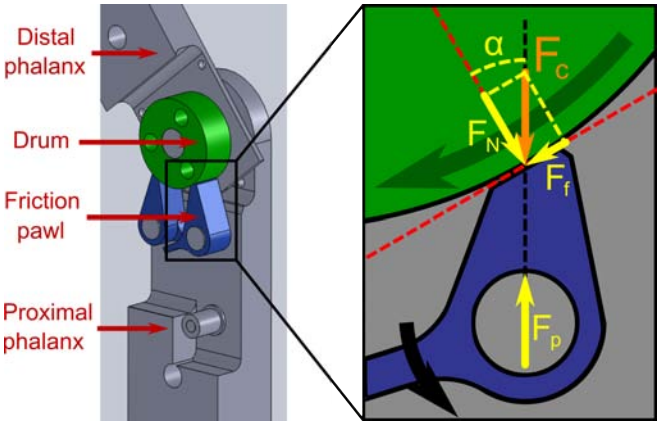

Fig. 4. Friction amplification concept. Once the friction pawl touches the drum, the joint becomes locked. The forces acting on the pawl are illustrated; curved arrows indicate the parts' direction of motion before locking.

of a material's ultimate tensile strength; therefore, hardened tool steel (45NiCrMo16, ISO 1.2767) with an ultimate tensile strength of around 1500 MPa has been selected.

B. Friction amplification

The joint torque can also be opposed by a friction-based locking mechanism, which uses rotating friction pawls to block the motion of a drum connected to the distal phalanx. This friction amplification (FA) mechanism can be seen in Figure 4. When one of the friction pawls is moved into contact with the rotating central drum, the friction between them pulls the pawl further along. This increases the contact force between drum and pawl, and thereby the friction. It should be noted this locking principle is unidirectional; two friction pawls would be needed to enable joint locking in both directions.

Design: The free body diagram describing the forces acting on the pawl during self-locking is shown in Figure 4. If the friction pawl is self-locking, it becomes a two-force member, meaning the line of the pawl shaft force F_p lies through both the rotation point and the contact point. This can only be the case if the angle α between this line and the normal force F_N is smaller than the friction angle $(\arctan(\mu))$. Similar to the gear concept, the contact angle should therefore be 20 degrees or lower.

Given the 1 Nm maximum joint torque and a drum diameter of 15 mm, the maximum friction force F_f will be approximately 133 N; at a 20 degree contact angle, this leads to a contact force F_c of approximately 365 N.

To determine the maximum contact stress, the pawl and drum are modeled as parallel cylinders. This leads to the following equations for the maximum Hertzian contact stress σ_{Hmax} [16], where F_c is the contact force, E is the Young's modulus of the material, ν is the Poisson ratio of the material, b is the width of the contact area, and ρ is based on the contact surfaces' radii of curvature ρ_1 and ρ_2:

$$\sigma_{Hmax} = \sqrt{\frac{1}{2\pi \cdot (1-\nu^2)} \cdot \frac{F_c \cdot E}{b \cdot \rho}}\,, \tag{5}$$

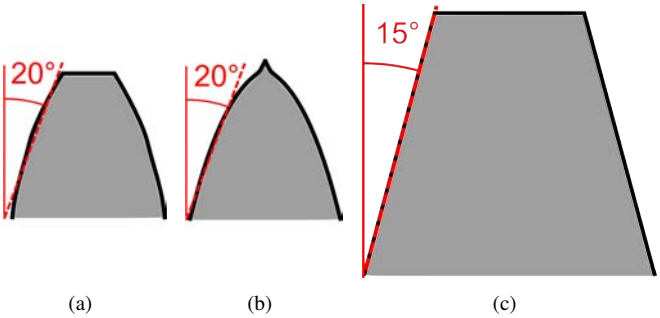

Fig. 5. Pawl tooth variations: (a) Involute teeth, used in pawls T1 and T2; (b) Pointed teeth, used in pawl T3; (c) Straight teeth, used in pawl T4. The tooth angle is indicated in red.

TABLE I

TOOTHED PAWL PARAMETERS.

Pawl	T1	T2	T3	T4
Number of teeth	10	2	10	2
Tooth angle (deg)	20	20	20	15
Gear module	0.2	0.2	0.2	0.5
Indexing resolution (deg)	3.6	3.6	3.6	9
Tooth shape	Involute	Involute	Pointed	Straight

$$\text{where } \rho = \frac{\rho_1 \cdot \rho_2}{\rho_1 + \rho_2} \tag{6}$$

Given steel-on-steel contact and a flat pawl surface, this results in a maximum contact stress of approximately 597 MPa. The hardened tool steel mentioned in Section III-A has an allowable contact stress of several thousand MPa, so this should not be a problem.

C. Actuation

Various methods of electrically powered small-scale actuation are currently available. The following have been investigated: piezo elements, shape memory alloy, and solenoids.

Many varieties of piezoelectric actuator are available, based on the deformation of certain materials when exposed to an electric field. A $5 \times 5 \times 18$ mm^3 piezoelectric stack actuator can provide forces in excess of 800 N, though its stroke is limited to around 0.015 mm [17]. This stroke can be raised to 1 mm by implementing a piezo bending actuator, which reduces the actuation force to a maximum of 0.5 N [18].

Shape memory alloy (SMA) is a material that when deformed can return to a previous shape when exposed to a change in temperature. This effect can be used in actuation, and requires only a wire of SMA material and an electrical current to heat it. The drawbacks of a SMA wire of sufficient size are a cooldown time of up to several seconds [19] and hysteresis in the transformation characteristic [20].

Solenoid actuators use an electromagnetic field to move a ferromagnetic armature. A solenoid actuator with a diameter of 11.3 mm and a length of 13.3 mm can exert impulse forces of up to 4.5 N with a stroke of 2 mm [21]. However, a higher stroke or longer operation time reduces the maximum force.

When comparing the above actuators, the solenoid actuator provides the best combination of actuation force and

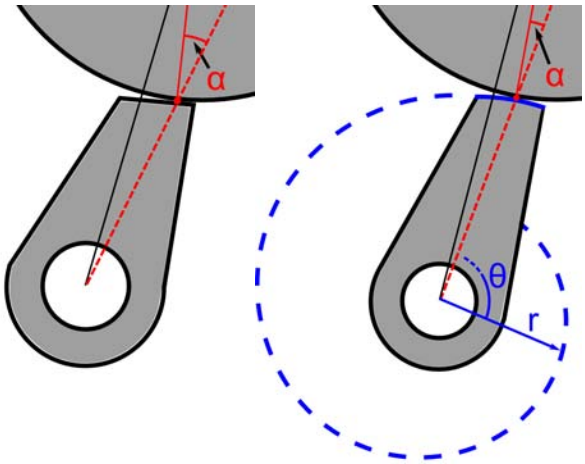

(a) (b)

Fig. 6. Friction pawl variations: (a) Short pawl with flat contact surface, used in pawls F1, F2, and F3; (b) Long pawl with spiraled contact surface, used in pawls F4, F5, and F6. The contact angle α is indicated in red; the spiral's radius r and angle θ are indicated in blue.

TABLE II
FRICTION PAWL PARAMETERS.

Pawl	F1	F2	F3	F4	F5	F6
Length (mm)	8.6	8.6	8.6	22.9	22.9	22.9
Contact angle (deg)	24	18	8	13	10	7
Contact surface	Flat	Flat	Flat	Spiral	Spiral	Spiral

stroke. Therefore, for further evaluation of the lock concepts solenoid actuation will be used.

IV. TESTING

To allow for uncertainties in the design parameters, several variations of each concept have been developed. In this section, these variations are described, followed by a test protocol based on the requirements.

A. Concept variations

The gear locking concept features four different gear wheel/pawl combinations (T1 through T4), with variations in the number of teeth on the pawl, tooth shape, and tooth size.

For the FA concept, six friction pawls have been made (F1 through F6) with varying contact angle α (see Figure 4). Also, two different implementations of the friction pawls' contact area have been tested: in addition to the default flat profile, a logarithmic spiral surface has been designed. The radius of these pawls' contact surface r depends on the angle θ as follows: $r = a \cdot e^{b\theta}$. At any point on this surface, the angle ϕ between the tangent and the radial line is constant and given by $\phi = \arctan(\frac{1}{b})$. This reduces the effect of play, as the pawl can accommodate variations in distance to the drum with minimal effect on the contact angle α. This concept is illustrated in Figure 7.

The respective parameters for each of the pawls can be found in Table I and Table II, and are illustrated in Figure 5 and Figure 6.

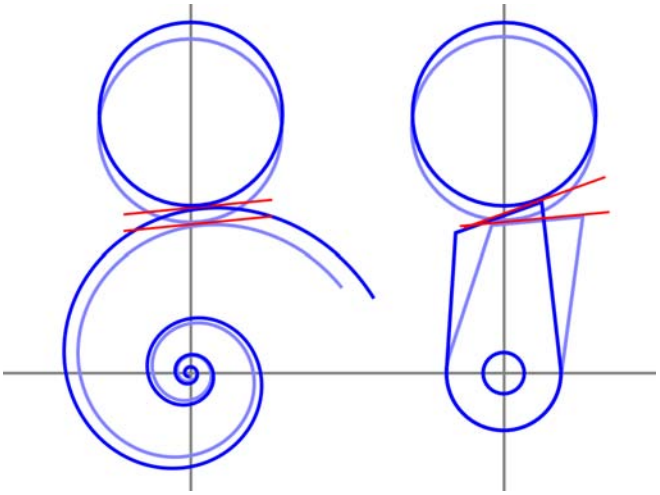

Fig. 7. A diagram illustrating the effect of play on the contact angles of a logarithmic spiral and a straight pawl.

B. Test protocol

For each of the systems described in Section IV-A, the following tests are performed:

Self-locking: First, the lock's self-locking properties are tested; the joint lock is actuated with a force of 10 N, and an external torque of 1 Nm is applied to the joint. As soon as the joint is successfully locked, the actuation force is removed. If the joint remains locked, it can be considered self-locking.

Torque ratio: If the lock is not self-locking, the ratio of maximum locking torque to actuation force will be determined. This is done by measuring the maximum torque the lock can withstand without slipping or releasing for different actuation forces.

Actuation and release: The pawl stroke required to engage and release the lock is evaluated, and if the lock is self-locking, the force required to release the lock is measured.

The test setup used for the gear locking and FA concepts can be seen in Figure 8.

V. RESULTS

Summaries of the test data for both concepts are shown in Table III and Table IV. For each test, the results are discussed separately.

A. Self-locking

No self-locking was observed for any of the gear-locking concepts. The FA concepts showed self-locking at contact angles of 10 degrees and lower, though the property was inconsistent when testing the 10 degree FA pawl (pawl F5). The self-locking FA concepts (pawls F3, F5, and F6) were able to handle joint torques up to 2.0 Nm without any problems.

B. Torque ratio

For the non-self-locking pawls, the ratio between the maximum locking torque and actuation force was measured. These can be seen in Table III and Figure 9 for the gear

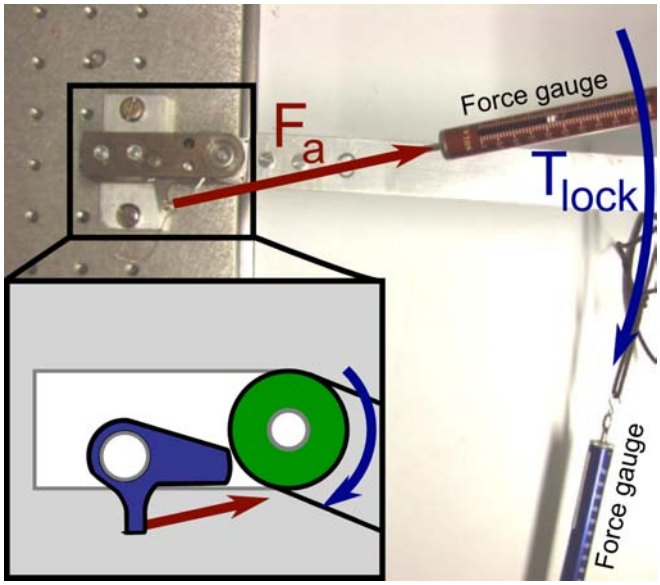

Fig. 8. Joint lock test setup, with a diagram of the internal mechanism of the FA concept. Actuation force (F_a), locking torque (T_{lock}), and the force gauges used to measure these are indicated.

concept, and Table IV for the FA concept. The gear concept showed an almost linear ratio, independent of movement direction or joint angle. During testing of the non-self-locking FA concepts, the torque ratio proved almost negligible. At the 10 degree contact angle (pawl F5), the self-locking property was observed to be dependent on joint orientation and applied actuation force, as seen in Figure 10.

C. Actuation and release

The gear wheel's actuation and release stroke depends on the geometry of the teeth, and the number of teeth on the pawl. For the two-toothed pawls, the stroke is equal to the tooth length; the ten-toothed pawls require a slightly larger stroke to clear the gear. As none of the toothed pawls are self-locking, no release force was measured.

Although the FA concept has almost zero actuation stroke, a significant amount of joint compliance was found with the spiraled self-locking pawls (F5 and F6); this caused up to 11 degrees of additional joint deflection at 1 Nm. Because of their low contact angle, any deformation or play in the lock components results in a large rotation of the locked joint; additionally, the spiraled surface of the pawls causes a slower buildup of force in the lock, leading to a lower rotational stiffness.

After removing the joint torque, the force required to release the self-locking FA systems was found to be approximately 0.3 N.

VI. Discussion

In this section, the differences in performance of the concept variations are discussed. Afterwards, the concepts will be evaluated by comparing the test results to the appropriate requirements.

TABLE III

Gear locking concept test results. Since no self-locking occurred, no release forces were measured.

Pawl	T1	T2	T3	T4
Self-locking	No	No	No	No
Torque ratio (Nm/N)	0.03	0.045	0.077	0.125
Actuation/release stroke (mm)	0.8	0.7	0.8	1.2

TABLE IV

Friction amplification test results. (*) indicates conditional self-locking.

Pawl	F1	F2	F3	F4	F5	F6
Self-locking	No	No	Yes	No	Yes*	Yes
Torque ratio (Nm/N)	~0	~0	N/A	0.006	0.015	N/A
Release force (N)	N/A	N/A	0.2	N/A	0.3	0.3

A. Concept variations

Gear locking: The decrease in tooth angle had a positive effect on the torque ratio. Also, reducing the number of teeth from 10 to 2 made it more likely for the pawls to lock into the gear wheel. Increased tooth size showed no obvious benefits, whereas the higher indexing resolution is a significant drawback. The pointed shape of the teeth on pawl T3 initially resulted in a higher locking torque, though the shape was worn down after several rounds of testing.

Friction amplification: For the FA concept, the variations in contact angle and contact surface shape were most influential. The locks' performance was almost exclusively reliant on the occurrence of self-locking, and the required contact angle for self-locking proved to be much lower than expected. The spiraled contact surface ensured that any play caused by the high normal forces had no effect on the contact angle, though it also resulted in an increase in compliance of the locked joint. Increasing the pawls' length also diminished the relative effects of play in the shafts and bearings.

B. Concept evaluation

Mechanism size and weight: The gear locking concept's gear wheel exceeded the stated joint size requirement by 3 mm. However, reducing the number of teeth to 75 could lower the diameter to 15 mm without exceeding 5 degrees of indexing resolution.

The thicknesses of the gear wheel and FA drum were 4 and 5 mm, respectively, which allows for the placement of actuation pulleys and extension springs in the joint.

An early prototype of the FA concept with solenoid actuator implemented in a $15 \times 17 \times 60$ mm^3 phalanx can be seen in Figure 11. The total weight of all lock components and the solenoid actuator is 17.2 g for the gear concept, and 13.4 g for the FA concept.

Actuation force and stroke: As mentioned in Section III-C, the selection of a solenoid actuator limits the actuation force to 4.5N. The test results show that none of the tested gear locking concepts would fulfil this requirement, as the minimal actuation force needed to meet the joint torque requirement of 1.0 Nm was 8 N. The actuation stroke of all concepts was less than the solenoid's 2 mm stroke.

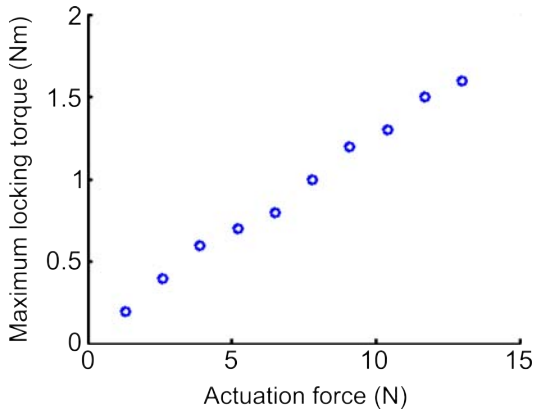

Fig. 9. Maximum locking torque as a function of actuation force for the gear locking concept, pawl T4.

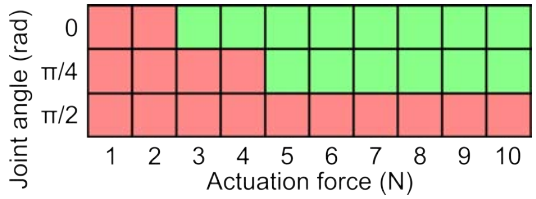

Fig. 10. The self-locking of FA concept 5 as a function of joint angle and actuation force; green squares represent self-locking, and red squares represent slippage.

For the FA concepts, the magnitude of the actuation force had little effect on the locking torque; the self-locking concepts required no actuation force, but the non-self-locking pawls required over 70 N to lock 1 Nm of joint torque.

Joint torques: Both concepts are capable of withstanding joint torques of 1 Nm, though the gear locks require an actuation force of more than 8 N; the self-locking FA concepts were found to withstand torques of up to 2 Nm without damage.

VII. Conclusions

In-phalanx joint locking mechanisms are a feasible way of improving the controllability of underactuated fingers. Though neither the small size of the mechanisms nor the high joint torques proved to be a problem in their development, the locks' actuation force was limited by the small space available for actuation. After testing both concepts, only some of the FA concepts were able to meet all requirements. This is mainly due to their capacity for self-locking, which is entirely absent from the tested gear locking concepts.

The concepts' self-locking capabilities depend mainly on the contact angle of the pawls and the friction coefficient of the materials. Since self-locking was only observed at contact angles below 10 degrees, the friction coefficient appears to lie below expected values. Lower contact angles also resulted in higher contact forces than expected, though the locks experienced no failures with joint torques of up to 2 Nm.

The gear concept can be improved by reducing the tooth angle, as well as investigating other tooth shapes for both locking torque and wear resistance. For the FA concept, joint compliance could be reduced by increasing the mechanism's friction and contact angle.

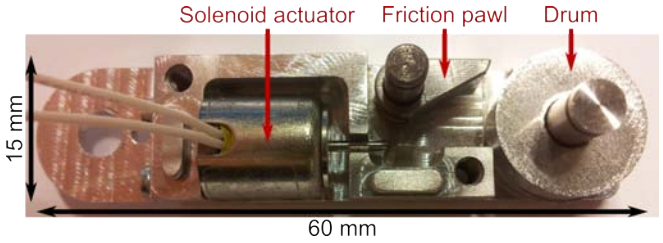

Fig. 11. Prototype of the FA joint lock concept with solenoid actuation, integrated in a human-sized phalanx.

For future work, four of the FA locks will be implemented in a two-fingered prosthesis prototype, to demonstrate a variety of grasp types with a single main actuator.

References

[1] RSLSteeper. bebionic. http://www.bebionic.com/.

[2] Touch Bionics Inc. i-LIMB Hand. [Online]. Available: http://www.touchbionics.com/i-LIMB

[3] Otto Bock. Michelangelo Hand. http://www.ottobock.com/.

[4] B. Peerdeman, D. Boere, H. Witteveen, R. Huis in 't Veld, H. Hermens, S. Stramigioli, J. Rietman, P. Veltink, and S. Misra, "Myoelectric forearm prostheses: State of the art from a user requirements perspective," *Journal of Rehabilitation Research & Development (JRRD)*, vol. 48, no. 6, pp. 719–738, July 2011.

[5] M. Saliba and C. de Silva, "An innovative robotic gripper for grasping and handling research," in *Proceedings of the International Conference on Industrial Electronics, Control and Instrumentation (IECON)*, vol. 2, 1991, pp. 975–979.

[6] N. Ulrich, V. Kumar, R. Paul, and R. Bajcsy, *Grasping with mechanical intelligence*. Warsaw, Poland: School of Engineering and Applied Science, University of Pennsylvania, 1989.

[7] J. U. Chu, D. H. Jung, and Y. J. Lee, "Design and control of a multifunction myoelectric hand with new adaptive grasping and self-locking mechanisms," in *Proceedings of the IEEE International Conference on Robotics and Automation*, 2008, pp. 743–748.

[8] J. Pons, E. Rocon, R. Ceres, D. Reynaerts, B. Saro, S. Levin, and W. van Moorleghem, "The MANUS-HAND dextrous robotics upper limb prosthesis: Mechanical and manipulation aspects," *Autonomous Robots*, vol. 16, no. 2, pp. 143–163, 2004.

[9] C. Light and P. Chappell, "Development of a lightweight and adaptable multiple-axis hand prosthesis," *Medical Engineering and Physics*, vol. 22, pp. 679–684, 2000.

[10] M. Carrozza, G. Cappiello, S. Micera, B. B. Edin, L. Beccai, and C. Cipriani, "Design of a cybernetic hand for perception and action," *Biological Cybernetics*, vol. 95, no. 6, pp. 629–644, 2006.

[11] B. Buchholz and T. J. Armstrong, "An ellipsoidal representation of human hand anthropometry," *Human Factors: The Journal of the Human Factors and Ergonomics Society*, vol. 33, pp. 429–441, 1991.

[12] T. J. Armstrong, C. Best, S. Bae, J. Choi, D. C. Grieshaber, D. Park, C. Woolley, and W. Zhou, "Development of a kinematic hand model for study and design of hose installation," pp. 85–94, 2009.

[13] S. Schulz, C. Pylatiuk, M. Reischl, J. Martin, R. Mikut, and G. Bretthauer, "A hydraulically driven multifunctional prosthetic hand," *Robotica*, vol. 23, no. 3, pp. 293–299, 2005.

[14] B. Dizioglu and K. Lakshiminarayana, "Mechanics of form closure," *Acta Mechanica*, vol. 52, pp. 107–118, 1984.

[15] B. Hamrock, S. Schmid, and B. Jacobson, *Fundamentals of machine elements*, ser. McGraw-Hill series in mechanical engineering. McGraw-Hill Higher Education, 2004.

[16] K. Johnson, *Contact mechanics*. Cambridge University Press, 1987.

[17] Piezo Systems, Inc. Piezo Stack Actuators. http://www.piezo.com/prodstacks1.html.

[18] ——. Piezo Bending Actuators. http://www.piezo.com/prodbm64l.html.

[19] P. Potapov and E. P. da Silva, "Time response of shape memory alloy actuators," *Journal of Intelligent Material Systems and Structures*, vol. 11, pp. 125–134, February 2000.

[20] W. J. Buehler and F. E. Wang, "A summary of recent research on the nitinol alloys and their potential application in ocean engineering," *Ocean Engineering*, vol. 1, no. 1, pp. 105–120, 1968.

[21] Geeplus Europe Ltd. C110 small push pull solenoid. [Online]. Available: http://www.geeplus.biz